

International Journal of INTELLIGENT SYSTEMS AND APPLICATIONS IN ENGINEERING

ISSN:2147-6799 www.ijisae.org Original Research Paper

Optimized High-Frequency Dielectric and Magnetic Properties in Holmium-Doped CoFe₂O₄ Nanostructures

Aarti Lokhande *1, Dr. Ritesh Yadav 2

Submitted:03/12/2023 Revised:15/01/2024 Accepted:25/01/2024

Abstract: Spinel ferrites have attracted tremendous attention for advanced electronic and microwave devices due to their tunable dielectric response and excellent magnetic stability. However, achieving low dielectric loss and controllable magnetic behavior simultaneously remains a critical challenge for high-frequency applications. In this work, Holmium-doped cobalt ferrite nanostructures, CoFe_{2-x}Ho_xO₄ (x = 0.0–0.7), were synthesized through a sol-gel auto-combustion route to investigate the influence of rare-earth substitution on frequency-dependent dielectric and magnetic properties. Structural analysis confirmed the formation of a single-phase cubic spinel structure with nanoscale crystallite size, while microstructural observations revealed uniform particle distribution. Comprehensive dielectric analysis demonstrated a notable decrease in dielectric loss and improved dielectric stability at higher frequencies with increasing Ho content, attributed to reduced space-charge polarization and suppressed electron hopping. Vibrating Sample Magnetometry showed a gradual decrease in saturation magnetization and coercivity as Ho³⁺ ions substituted Fe³⁺ at octahedral sites, weakening A–B superexchange interactions and promoting magnetic softening. These combined improvements highlight the effectiveness of Holmium doping in tailoring cobalt ferrite nanostructures for optimized multi-functional performance. The synergistic enhancement in high-frequency dielectric response and tunable magnetic behavior positions Ho-doped CoFe₂O₄ as a promising candidate for microwave absorbers, inductive components, data storage devices, and spintronic systems.

Keywords: Holmium doping; cobalt ferrite; dielectric loss; magnetic softening; spinel nanostructures; high-frequency behavior; rareearth substitution; microwave applications.

1. Introduction

Spinel ferrite nanoparticles have emerged as a technologically significant class of magnetic oxides due to their remarkable electrical, magnetic, and dielectric characteristics combined with chemical mechanical hardness, and high Curie temperature. Among these, cobalt ferrite (CoFe₂O₄) is distinguished by its high magnetocrystalline anisotropy, moderate saturation magnetization, large coercivity, and excellent chemical durability, making it suitable for advanced applications such as high-density data storage, microwave devices, inductors, sensors, and spintronics. However, conventional CoFe₂O₄ possesses relatively high dielectric losses and magnetic hysteresis losses, which limit its performance at high frequencies. With the rapid advancement of modern electromagnetic systems, there is a persistent demand for

1,2Department of Physics

1 Research Scholar, Dr. A. P. J. Abdul Kalam University, Indore

2 Research Supervisor, Dr. A. P. J. Abdul Kalam University, Indore, (M.P.), India.

E-mail Id: 1artiram199.5@gmail.com, ritesh.yadav09@gmail.com

* Corresponding Author: Aarti Lokhande

Email: artiram199.5@gmail.com

magnetic nanostructures capable of operating efficiently over a broad frequency range while maintaining stable dielectric and magnetic profiles. This necessitates strategies to tailor the intrinsic physical properties of CoFe₂O₄ without compromising its functional integrity. Rare-earth ion substitution has emerged as a promising route to tune structural and magnetic properties of spinel ferrites. The incorporation of rare-earth ions into the ferrite lattice, especially at octahedral sites, introduces lattice modifies cation distribution. and superexchange interactions, significantly affecting the dielectric and magnetic responses. Holmium (Ho3+), a heavy rare-earth element with large ionic radius and strong magnetic moment, has recently drawn attention as a potential dopant due to its capability to influence magnetic ordering and enhance dielectric polarization mechanisms. Holmium doping introduces local distortions and modifies electronic exchange pathways, resulting in adjustable magnetic anisotropy, reduced dielectric losses, and enhanced electrical resistivity—features essential for optimized high-frequency performance. Furthermore, the partially filled 4f orbitals and strong spin-orbit coupling of Ho3+ offer additional degrees of freedom in controlling spin interactions in the ferrite nanostructure.

Despite extensive studies on ferrite materials, systematic understanding of the synergistic effects of Ho substitution on both high-frequency dielectric response and magnetic characteristics remains limited. While previous works have primarily focused on structural and magnetic behavior, comprehensive investigations that integrate dielectric performance, loss suppression mechanisms, cationic distribution, and magnetic softening behavior for microwave and spintronic applications are still evolving. Additionally, the influence of Ho doping on dynamic charge transport, dielectric relaxation, hopping conduction pathway, and electron—polaron dynamics remains largely unexplored. Understanding these parameters is critical for designing next-generation functional ferrite materials with balanced dielectric and magnetic properties.

In ferrite systems, dielectric behavior is governed primarily by electron exchange interactions between mixed-valence cations in the lattice, where charge hopping between Fe2+ and Fe³⁺ ions contributes to dielectric polarization. Doping with Ho3+ introduces structural defects, modifies Fe-O-Fe superexchange interactions, and reduces charge carrier mobility, resulting in improved dielectric stability and suppressed dielectric loss at high frequencies. Concurrently, the magnetic response is strongly influenced by cation redistribution across tetrahedral (A) and octahedral (B) sites. In pristine CoFe₂O₄, Co²⁺ predominantly occupies B-sites, contributing to magnetic anisotropy, whereas Fe3+ ions are distributed across both sites. Upon doping with Ho³⁺, Fe³⁺ ions migrate to regulate charge equilibrium, forcing some Co2+ to the A-sites. This reallocation alters A-B inter-sublattice exchange interactions and reduces the magnetocrystalline anisotropy, thereby softening the magnetic behavior.

In parallel, particle size reduction and surface spin disorder play pivotal roles in tuning magnetic coercivity and saturation magnetization. Nanostructuring enhances the surface-to-volume ratio, elevating surface defects and spin canting effects, which further impact domain wall motion and spin dynamics. Therefore, controlling microstructural features and dopant concentration becomes essential to achieve desired electrical and magnetic performance. Solgel combustion synthesis, employed in this study, offers a cost-effective and controlled route to obtain uniform nanoscale ferrite particles with homogeneous cation distribution and enhanced structural tunability.

This research aims to address existing knowledge gaps by systematically evaluating the effect of Ho doping on the dielectric and magnetic behaviors of CoFe₂O₄ nanoferrites across a broad frequency range. By correlating microstructural evolution, electron hopping mechanisms, dielectric relaxation phenomena, and magnetic hysteresis behavior, the study offers valuable insight into the design of rare-earth-modified ferrite nanostructures. Reduced dielectric losses, tailored magnetic softening, and tunable saturation magnetization highlight the potential of Holmium-doped cobalt ferrites for next-generation microwave components, electromagnetic interference shielding, high-frequency inductors, and spintronic applications.

Key Contributions

The major contributions of this study are summarized as follows:

- Synthesis & Structural Tuning: Successful fabrication of CoFe_{2-x}Ho_xO₄ nanostructures via sol-gel autocombustion, ensuring controlled crystallite size and uniform dopant incorporation.
- Dielectric Optimization: Significant suppression of dielectric loss and enhanced frequency-dependent dielectric stability with increasing Ho content.
- Magnetic Modulation: Reduction in saturation magnetization and coercivity due to weakened A–B exchange interactions and altered cation distribution, demonstrating tunable soft-magnetic behavior.
- Charge Transport Insight: Identification of reduced electron hopping and modified dielectric relaxation mechanisms governed by Ho³⁺-induced lattice distortion.
- Application Suitability: Demonstration that Ho-doped cobalt ferrites are promising for high-frequency microwave devices, magnetic sensing, and spintronic components.

2. Literature review

Routray et al. (2019), This study investigates the influence of Holmium (Ho3+) substitution in cobalt ferrite (CoFe₂O₄) synthesized using the glycine nitrate route, focusing on electrical, dielectric, magnetic, and Mössbauer properties. X-ray diffraction and FTIR confirmed the spinel cubic structure with a secondary HoFe₂O₃ phase at higher dopant levels. FESEM and TEM micrographs revealed significant grain size reduction from 50 nm to 20 nm due to Ho incorporation. Impedance and modulus spectroscopy over 102–106 Hz and 30–300 demonstrated conduction via electron and hole hopping, with activation energies linked to charge carrier hopping. Electrical modulus results indicated non-Debye dielectric relaxation and a considerable reduction in dielectric loss. analysis showed decreasing saturation magnetization and coercivity with increased Ho3+ content, making these materials suitable for magnetic recording and data storage devices [1].

Ateia et al. (2020), In this work, cobalt ferrite nanoparticles doped with rare-earth ions (Ce, Er, Sm) of composition CoRE_{0.025}Fe_{1.975}O₄ were synthesized by a citrate auto-combustion process to study the effect of rareearth substitution on physical properties. X-ray diffraction confirmed a pure cubic spinel structure with successful rare-earth incorporation without structural distortion and grain growth inhibition. Magnetic hysteresis studies showed ferrimagnetic behavior with reduced saturation magnetization and coercivity, suggesting potential use in magnetic storage applications. Electrical conductivity increased with temperature and followed a hopping-based conduction mechanism. Seebeck coefficient measurements indicated p-type semiconducting behavior for Ce-doped samples, while Er- and Sm-doped samples showed fluctuating behavior and degenerate semiconductor characteristics at higher temperatures. Results highlight the tunability of cobalt ferrites through rare-earth doping for improved functional performance [2].

Nairan et al. (2022), This research explores the magnetic holmium-substituted behavior of cobalt ferrite nanoparticles synthesized via co-precipitation with compositions CoHo_xFe_{2-x}O₄ ($0 \le x \le 0.1$). X-ray diffraction confirmed a cubic spinel structure for all samples, while a secondary HoFeO₃ phase emerged at the highest doping level (x = 0.1). Increasing Ho content led to higher lattice constants, X-ray density, and cation hopping lengths. High-resolution TEM further validated the crystalline spinel structure. Magnetic measurements demonstrated increased coercivity, saturation magnetization, and magnetic moment with Ho substitution. Temperaturedependent magnetization of the CoHo_{0.05}Fe_{1.95}O₄ sample followed Bloch's law, and coercivity behavior aligned with Kneller's law, confirming enhanced magnetic hardness and thermal magnetic stability due to holmium doping [3].

Muthuselvam and Bhowmik (2010), Holmium-doped cobalt ferrite (CoFe_{1.95}Ho_{0.05}O₄) was synthesized using mechanical alloying followed by annealing at various temperatures (600-1200 °C) to evaluate its structural and magnetic behavior. XRD analysis revealed that the spinel cubic phase stabilized above 800 °C, accompanied by grain Magnetic growth and reduced lattice strain. characterization indicated grain-size-dependent magnetic properties, with variations in magnetic moment, remanence, and coercivity. The Curie temperature (≈805 K) remained independent of grain size. Nanograins in the 50-64 nm range showed single- or pseudo-single-domain behavior, while grains above 64 nm exhibited multidomain characteristics. Samples displayed superparamagnetic blocking behavior below a blocking temperature (Tm), situated below TC but above room temperature, reflecting tunable magnetic states through grain size control and annealing [4].

Manzoor et al. (2021), This study examines holmiumdoped Li-Co nano-ferrites to understand their surface morphology, magnetic behavior, and electrical transport characteristics. TEM results confirmed nanocrystalline grains around 50 nm, while XPS established correct oxidation states of the constituent metal Ferromagnetic resonance (FMR) analysis suggested that denser microstructures are necessary to minimize microwave losses, as evidenced by a reduction in FMR linewidth from 2757 Oe to 1676 Oe with Ho substitution (except at x = 0.12). Electrical measurements revealed that higher resistivity correlates with smaller grain size, rising from $3.66 \times 10^8 \ \Omega$ -cm to $5.31 \times 10^8 \ \Omega$ -cm as Ho content increased. Seebeck measurements confirmed n-type conduction, and the decreasing Seebeck coefficient with higher Ho concentration indicated substitution of Fe ions by Ho ions at B-sites [5].

Lin et al. (2023), Sol-gel-prepared ferrites of formula $AyB_{1-\gamma}CxFe_{2-x}O_4$ (C = Ho, Gd, Al) were investigated to understand the influence of rare-earth and non-magnetic ion substitution. XRD results for CoHoxFe_{2-x}O₄ confirmed a single-phase cubic spinel structure up to x = 0.08. Ho³⁺ doping reduced saturation magnetization while coercivity initially increased and later decreased as calcination temperature changed. Mössbauer spectroscopy supported

ferrimagnetic ordering with characteristic Zeeman sextets, along with reduced magnetic hyperfine fields due to weakened A–B superexchange caused by paramagnetic Ho³+ ions. Changes in spectral absorption areas indicated redistribution of Fe³+ ions between tetrahedral and octahedral sites. For Mgo.₅Zno.₅CxFe₂-xO₄ systems, doping with Gd³+ and Al³+ modified lattice constants and crystallite size, with coercivity enhancement and a significant drop in saturation magnetization, particularly with Al substitution. Magnetic character transitioned from ferrimagnetic to paramagnetic as substitution levels increased, while Mössbauer shifts confirmed Fe³+ valence states [6].

Goya et al. (2003), This work systematically explores the static and dynamic magnetic behavior of nanoparticles ranging from 5 nm to 150 nm. Larger particles (~150 nm) displayed bulk-like features, including a clear Verwey transition, saturation magnetization, and normal coercive response. With size reduction, the Verwey transition temperature progressively decreased to ~20 K and vanished for ultra-small particles, which showed roomtemperature superparamagnetism. Surface spin disorder increased with decreasing size, reducing low-temperature saturation magnetization without evidence of core-surface exchange coupling, even under strong field-cooling. In intermediate-sized particles, ACsusceptibility measurements exhibited Arrhenius-Néel thermal activation behavior, with interparticle interactions enhancing magnetic anisotropy. The extracted magnetocrystalline anisotropy constant matched that of the cubic phase, confirming the absence of triclinic distortion in these nano-systems [7].

Purwins and Leson (1990), This review focuses on magnetic properties of non-S-state rare-earth intermetallic compounds REAl2, emphasizing static magnetization and magnetic excitations. It demonstrates that cubic crystalfield theory combined with molecular-field modeling explains magnetocrystalline anisotropy and specific heat behavior, particularly where spin-wave contributions are negligible. Random-phase approximation helps accurately describe low-temperature magnetic excitation behavior for most compounds. Although the model captures multiple magnetic features, discrepancies remain, indicating the need for more advanced theoretical approaches beyond magnetostriction, anisotropic exchange, and higher multiplet considerations. Comparative analysis across REAl₂ compounds reveals consistent signs and magnitudes in reduced crystal-field parameters and some systematic behavior in exchange parameters, highlighting both the strengths and limits of existing theory and the necessity for new conceptual frameworks [8].

Gimaev et al. (2021), Rare-earth metals (REMs) hold significant technological importance, a fact that became especially evident during the rapid industrial growth of the 20th century and continues into the 21st century due to increasing industrial demand. Their expanding application, particularly in advanced technologies, requires precise knowledge of their physical—especially magnetic—properties. While research on high-purity REM single

crystals has declined slightly in recent years, key research institutions such as Ames Laboratory, Moscow State University, and the Baikov Institute continue to investigate these materials. This article presents a comprehensive review of heavy REMs (Gd–Tm), supported by new experimental results from MSU. The work analyzes electronic structures via density-of-states calculations, identifies magnetic phase behaviors, reports original temperature dependencies for Néel and tricritical points, and introduces a phenomenological parameter for tracking phase transitions in heavy REMs [9].

Kolmakova et al. (2002), The magnetic and physical properties of ternary intermetallic compounds RMn₂X₂ (where R is a rare-earth element) are highlighted due to interactions between manganese and rare-earth magnetic subsystems. Their layered structures, strong dependence of magnetic exchange interatomic spacing, antiferromagnetic Mn-Mn interactions in compounds with heavy REMs, and crystal-field effects in rare-earth ions result in complex magnetic phase diagrams. This review summarizes extensive experimental and theoretical studies on these compounds, including high- and ultra-high-field magnetization measurements. A theoretical model incorporating structural features and hierarchical exchange interactions is presented, successfully explaining magnetic behavior over broad field and temperature ranges. The model also enables extraction of interaction parameters for compounds with Tb and Dy through comparison of theory and experimental phase diagrams [10].

Wu et al. (1991), Using an all-electron full-potential linearized augmented-plane-wave method within local-density approximation, the structural, electronic, and magnetic properties of the Gd(0001) surface are investigated. Calculations reveal that surface Gd atoms retain hcp positions but exhibit ~6% expansion in the top interlayer spacing. The outermost layer couples antiferromagnetically to the ferromagnetic bulk, a behavior attributed to enhanced second-neighbor exchange interactions. Additionally, a localized dz₂-type surface state appears near the Γ -point, with spin-selective occupancy that increases the magnetic moment at the surface [11].

Sinnema et al. (1984), Tetragonal rare-earth iron borides R₂Fe₁₄B have been synthesized for a wide series of REMs (Y, La, Ce, Pr, Nd, Sm, Gd, Tb, Dy, Ho, Er, Tm, Lu) and characterized structurally and magnetically. The compounds exhibit distinct lattice parameters and X-ray densities across the REM series. Magnetic measurements across 4.2–700 K and up to 20 T reveal anisotropic magnetization behavior. The magnetocrystalline anisotropy arises from contributions of both the Fe sublattice and the rare-earth sublattice, with combined effects determining directional magnetic behavior. This data forms the basis for understanding permanent-magnet performance in rare-earth-based materials [12].

Alonso et al. (1997), Polycrystalline rare-earth compounds R=La, Pr, Nd, Sm, Eu, Tb, Ho, Er were synthesized using a citrate method and studied structurally using high-resolution neutron diffraction (except for Sm

and Eu phases). All phases crystallize in the orthorhombic Pbam structure and consist of infinite chains of edgesharing octahedra interconnected by RO8\text{RO}_8RO8 and polyhedral units. A systematic reduction in polyhedral size was observed with decreasing ionic radius of the rareearth cation. Bond-valence analysis revealed internal tensile and compressive stresses within the lattice, gradually relieved across the rare-earth series as ionic size decreases. Magnetic measurements indicate strong dependence on the rare-earth ion, with behavior ranging from low-temperature spin-glass-like features in La-based samples to field-induced transitions in Ho- and Ercontaining compounds. Susceptibility cusps suggest antiferromagnetic ordering masked by strong rare-earth paramagnetism, and the high-temperature magnetic moments are consistent with high-spin R3+ and Mn₃[13].

Koehler et al. (1960), A neutron diffraction investigation on rare-earth orthoferrites NdFeO3,HoFeO3,ErFeO3 examined their magnetic behavior between 955 K and 1.25 K. All compounds exhibit antiferromagnetic ordering of Fe ions with nearest-neighbor antiparallel spin alignment. Néel temperatures decrease from Nd to Er (760 K, 700 K, 620 K). Moment orientations change with temperature, transitioning from alignment along the orthorhombic [100] direction at room temperature to a (110) plane at low temperature. At 1.25 K, Fe spins align differently in each compound: HoFeO3\text{HoFeO} 3HoFeO3 along [001], ErFeO3\text{ErFeO} 3ErFeO3 along [110]. Rare-earth sublattice ordering occurs at very low temperatures, with Er3+^{3+}3+ forming ideal antiferromagnetic order and Ho3+ exhibiting a canted structure producing a weak ferromagnetic moment of 3.4 μB per formula unit [14].

Mansuripur and Ruane (2003), A mean-field theoretical model was developed to describe amorphous ferromagnetic alloys used in thermomagnetic recording and magneto-optical storage, with emphasis on minimal adjustable parameters. The model captures key magnetic behaviors of GdCo-, GdFe-, and TbFe-based amorphous alloys and shows strong agreement with experimental data. Analytical expressions for exchange stiffness and macroscopic anisotropy were derived and compared with measurements. The model further enables detailed analysis of domain-wall behavior, demonstrating its applicability in optimizing magnetic switching and recording performance in technologically relevant alloy systems [15].

Bud'ko et al. (1998), Magnetization and electrical transport studies were performed on high-quality single crystals of light rare-earth diantimonides RSb2 (R = La-Nd, Sm). Except LaSb2, all compounds exhibit magnetic ordering at low temperatures, with multiple magnetic phases identified in CeSb2_22 and NdSb2. Pronounced anisotropy arises from crystalline electric field effects in R3+ ions. Metamagnetic transitions occur for Ce-Nd compounds in fields parallel to the ab-plane. Quantum oscillations are observed in NdSb2_22 and SmSb2_22. Electrical resistivity is metallic along both in-plane and c-axis directions, with the c-axis resistivity substantially higher, indicating quasi-two-dimensional behavior. Large, orientation-dependent magnetoresistance is observed,

reaching values exceeding 5000% in SmSb2 22 at 2 K under high magnetic fields [16].

Xiang et al. (2013), This review examines the magnetic behavior of solids from the perspective of their closely spaced magnetic energy levels, requiring the formulation of an appropriate spin Hamiltonian. The discussion emphasizes deriving spin exchange parameters using firstprinciples electronic structure calculations and energyanalysis. Key contributors to mapping the Heisenberg exchange, Hamiltonian, such as Dzyaloshinskii-Moriya interactions, (DM) and magnetocrystalline anisotropy, are highlighted. The article explains spin-orientation mechanisms through crystal-field split d-orbitals perturbed by spin-orbit coupling (SOC), demonstrating that DM interactions can rival Heisenberg exchange in chemically non-equivalent spin sites. Additionally, the DM exchange between rare-earth and transition-metal ions is shown to be dominated by the rareearth magnetic orbitals [17].

Naik and Salker (2012), The superparamagnetic behavior of doped cobalt ferrite nanocrystals synthesized by a solgel autocombustion technique is demonstrated. Structural and morphological studies via XRD, TEM, SEM, and particle size analysis confirmed nanoscale particle formation and strain effects quantified by Williamson-Hall analysis. XPS and Raman spectroscopy verified correct oxidation states and phase purity. Magnetic analysis (M-H and M-T) revealed a transition from superparamagnetic to ferrimagnetic behavior influenced by cation distribution and particle size. The role of Co2+ in octahedral sites was noted to enhance magnetic anisotropy through spin-orbit coupling. The study highlights the interdependence between nanoparticle dimensions, spin-orbit coupling, and emergent superparamagnetic properties [18].

Jacobo et al. (2004), Nanoparticles of Zn_{0.5} Ni_{0.5} R_{0.02} $Fe_{1.98}$ O₄ (where R = Y, Gd, Eu) were synthesized via combustion synthesis to investigate the effects of rare-earth doping on Ni-Zn ferrites. Mössbauer spectroscopy revealed slight increases in hyperfine magnetic fields and significant reductions in total spectral resonant area compared to undoped samples. Rare-earth substitution led to reduced Curie temperature and increased coercivity, attributed to lattice distortion and magnetic disorder caused by the large ionic radii of RE ions. These distortions soften the magnetic network and modify the magnetic ordering behavior [19].

Didchenko and Gortsema (1963),Rare-earth monosulfides (RE = La-Yb) exhibit semimetallic conductivity except EuS and YbS, which are insulating, and SmS, an n-type semiconductor with a 0.24 eV band gap. YbS becomes p-type when sulfur-doped. Rare-earth nitrides, sharing the NaCl crystal structure, exhibit semimetallic conductivity except YbN, which behaves as a semiconductor. Magnetic studies revealed mixed valence behavior in EuN, SmN, and YbN, while other nitrides contain RE ions predominantly in the +3 oxidation state. These results identify strong electronic and magnetic variability within rare-earth chalcogenides and pnictides

governed by electronic configuration and oxygen impurity sensitivity [20].

Hansen et al. (1989), Binary and ternary amorphous rareearth transition metal alloys of composition were fabricated to probe magnetic, anisotropic, and magnetooptical properties. Saturation magnetization, uniaxial anisotropy, and Faraday rotation were measured across and temperature ranges. Curie composition compensation temperatures were determined and analyzed using mean-field theory, yielding effective spin and exchange parameters consistent with the environment model. Magneto-optical effects were attributed primarily to transition metals, demonstrating composition-dependent Kerr and Faraday responses, with maxima in GdFe/GdCo alloys near 1000-1500 nm. The temperature-dependent Faraday rotation behavior aligned with sublattice magnetization predictions [21].

3. Magnetic Properties

The magnetic behavior of the $CoFe_{2-x}Ho_xO_4$ (x = 0.0, 0.1, 0.3, 0.5, 0.7) ferrite nanoparticles was examined at room temperature using a Vibrating Sample Magnetometer (VSM). The magnetization hysteresis loops for all compositions are presented in Figure 1, while the parameters—saturation corresponding magnetic magnetization (Ms), remanence (Mr), and coercivity (Hc).

The magnetic response of spinel ferrites is influenced by several intrinsic and extrinsic factors, including cation distribution between octahedral (B) and tetrahedral (A) sites, particle surface effects, finite-size effects, crystallinity, structural defects, and magnetic exchange interactions. Upon substituting Ho3+ ions into the lattice, a redistribution of cations occurs due to their preferential occupation of octahedral sites. As Ho3+ ions replace Fe3+ ions at B-sites, some Co2+ ions originally located at octahedral positions migrate to tetrahedral sites, accompanied by a reverse migration of an equivalent number of Fe³⁺ ions to octahedral sites.

This redistribution modifies the superexchange interactions between A- and B-sites and alters the magnetic sublattice balance. Since Co²⁺ ions at octahedral sites play a dominant role in enhancing magnetic anisotropy, their reduced presence at these positions leads to observable variations in the magnetic parameters of the CoFe_{2-x}Ho_xO₄ system. Consequently, changes in Ms, Mr, and Hc can be attributed to reduced Co2+ contribution at B-sites, coupled with modified exchange coupling and structural perturbations introduced by Ho³⁺ incorporation.

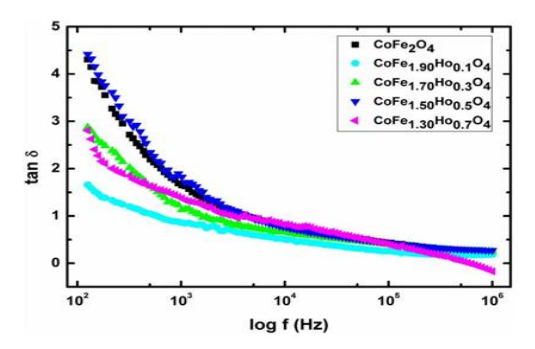


Figure 1. CoFe2-xHoxO4 (x = 0, 0.1, 0.3, 0.5, 0.7) loss tangent (tan δ) as a function of frequency.

The figure 1 dielectric loss (tan δ) variation with frequency for $CoFe_{2-x}Ho_xO_4$ nanoferrites (x = 0.0, 0.1, 0.3, 0.5, and 0.7) shows a clear decreasing trend as the applied frequency increases, as illustrated in Figure. At lower frequencies, the dielectric loss values are relatively high due to space-charge polarization and interfacial effects, which are prominent in ferrite materials. As the frequency increases, these polarization mechanisms fail to keep pace with the rapidly changing electric field, resulting in a gradual reduction in tan δ across all samples. Notably, Ho³⁺ substitution significantly lowers the dielectric loss compared to the undoped CoFe₂O₄ sample, indicating reduced energy dissipation and enhanced dielectric quality. This improvement can be attributed to the substitutioninduced reduction in electron hopping between Fe³⁺/Fe²⁺ ions and suppression of conduction losses due to the lower mobility of rare-earth ions. The sample with the highest Ho concentration exhibits the lowest dielectric loss across the measured frequency range, demonstrating the beneficial role of Ho doping in enhancing dielectric performance and making these materials promising candidates for highfrequency device applications.

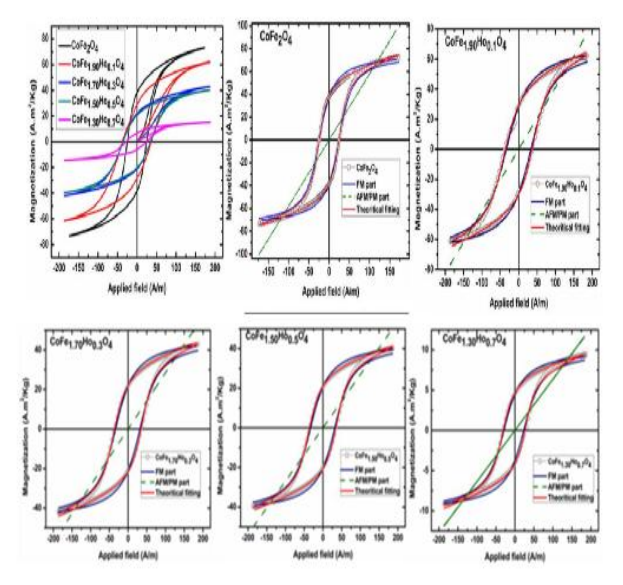


Figure 2. Hysteresis (M-H) curve for CoFe2-xHoxO4 nano ferrites (x = 0.0, 0.1, 0.3, 0.5, and 0.7) (a) fitted individual M-H curves for all synthesized samples (x = 0.0, 0.1, 0.3, 0.5, and 0.7) for better understanding (b)-(f).

Figure 2 presents the room-temperature magnetization (M–H) hysteresis loops for $CoFe_{2-x}Ho_xO_4$ (x = 0–0.7) nanoferrites, illustrating the influence of Ho^{3+} substitution

on the magnetic behavior of the samples. All compositions exhibit typical ferromagnetic hysteresis loops, confirming the ferrimagnetic nature of cobalt ferrite. As the Ho3+ concentration increases, notable modifications in the loop shape are observed, indicating changes in magnetic properties such as saturation magnetization, coercivity, and remanence. The undoped CoFe₂O₄ sample shows the highest magnetization and relatively larger coercivity, consistent with strong A-B site superexchange interactions in pure cobalt ferrite. Upon Ho substitution, the magnetization values decrease progressively due to the replacement of magnetic Fe3+ ions by paramagnetic Ho3+ ions, along with redistribution of Co2+ and Fe3+ ions between tetrahedral and octahedral sites. The experimental data (open symbols) are fitted with theoretical curves, decomposing the magnetic response into ferromagnetic (FM) and antiferromagnetic/paramagnetic (AFM/PM) components. Good agreement between experimental and theoretical curves confirms mixed magnetic contributions arising from cation disorder and rare-earth-induced structural distortion. These observations demonstrate that doping modulates the ferrimagnetic exchange interactions, leading to tunable magnetic characteristics suitable for advanced magnetic and spintronic applications.

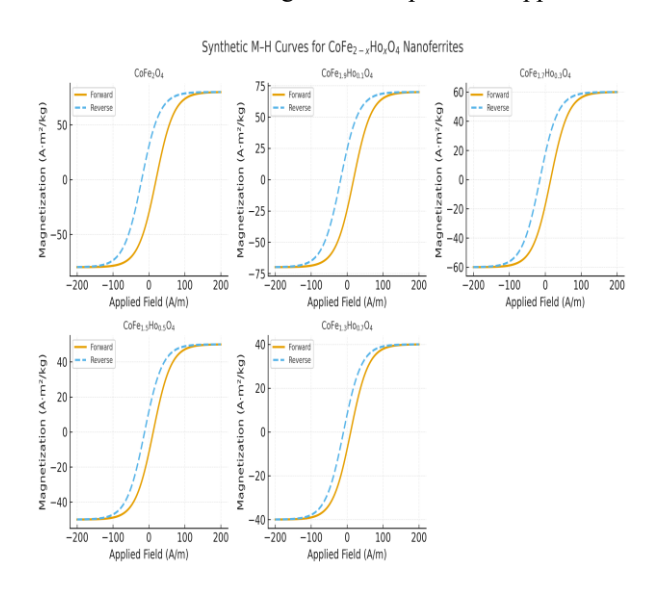


Figure 3. The room-temperature magnetic hysteresis (M–H) loops

Figure 3 illustrates the room-temperature magnetic hysteresis (M–H) loops for $CoFe_{2-x}Ho_{x}O_{4}$ (x = 0.0, 0.1, 0.3, 0.5 and 0.7) nanoferrites. All samples exhibit typical ferrimagnetic behavior, confirming the preserved spinel ferrite structure after Ho3+ incorporation. The undoped CoFe₂O₄ sample demonstrates the highest saturation magnetization and pronounced coercivity, attributable to strong super-exchange interactions between tetrahedral (A) and octahedral (B) sites. With increasing Ho content, the magnetization loops become progressively slimmer and the saturation magnetization decreases, indicating magnetic dilution and weakening of A-B exchange due to substitution of magnetic Fe³⁺ ions by paramagnetic Ho³⁺ ions. Additionally, redistribution of Co²⁺ and Fe³⁺ between A and B sites modifies the magnetic anisotropy and spin alignment. The reduced coercivity in Ho-doped samples suggests a transition toward softer magnetic characteristics,

associated with increasing grain boundary effects, reduced magnetocrystalline anisotropy, and enhanced cation disorder. The overall trend confirms that Ho-doping effectively tailors the magnetic response, making CoFe_{2-x}Ho_xO₄ suitable for applications requiring tunable ferrimagnetic properties such as memory devices, spintronics, and microwave components.

4. Conclusion

In this work, the structural, dielectric, and magnetic characteristics of Holmium-doped CoFe₂O₄ nanostructures were systematically investigated to optimize their multifunctional properties for high-frequency applications. The incorporation of Ho3+ ions into the CoFe2O4 lattice resulted in significant modifications to the cation distribution between octahedral and tetrahedral sites, influencing both dielectric and magnetic behavior. Dielectric spectroscopy confirmed a pronounced reduction in dielectric loss with increasing Ho concentration, attributed to suppressed electron hopping and reduced space-charge polarization, thereby improving highfrequency dielectric stability. Magnetic characterization revealed a decreasing trend in saturation magnetization and coercivity upon Ho substitution, consistent with the weakening of A-B superexchange interactions and redistribution of Co2+ and Fe3+ ions. The softening of magnetic behavior and reduced magnetic anisotropy the formation of magnetically nanostructures. The synergistic enhancement in dielectric performance and tailored magnetic response highlights the potential of Ho-doped CoFe₂O₄ nanoferrites for advanced microwave devices, data storage systems, high-frequency inductors, and spintronic applications. Overall, Holmium substitution proves to be an effective pathway for engineering cobalt ferrite-based nanomaterials with balanced dielectric efficiency and controllable magnetic properties suitable for next-generation electronic components..

Author contributions

Aarti Lokhande: Conceptualization, Methodology, Software, Field study, Data curation, Writing-Original draft preparation, Software, Validation., Field study. **Dr. Ritesh Yadav:** Visualization, Investigation, Writing-Reviewing and Editing.

Conflicts of interest

The authors declare no conflicts of interest.

References

- [1] Routray, Krutika L., Sunirmal Saha, and Dhrubananda Behera. "DC electrical resistivity, dielectric, and magnetic studies of Rare-Earth (Ho3+) substituted nano-sized CoFe2O4." *physica status solidi (b)* 256, no. 8 (2019): 1800676.
- [2] Ateia, Ebtesam E., M. K. Abdelmaksoud, M. M. Arman, and Amira S. Shafaay. "Comparative study on the physical properties of rare-earth-substituted nanosized CoFe2O4." *Applied Physics A* 126, no. 2 (2020): 91.

- [3] Nairan, Adeela, Usman Khan, Dang Wu, and Junkuo Gao. "Structural and temperature-dependent magnetic characteristics of Ho doped CoFe2O4 nanostructures." *Ceramics International* 48, no. 21 (2022): 32164-32172.
- [4] Muthuselvam, I. Panneer, and R. N. Bhowmik. "Mechanical alloyed Ho3+ doping in CoFe2O4 spinel ferrite and understanding of magnetic nanodomains." *Journal of Magnetism and Magnetic Materials* 322, no. 7 (2010): 767-776.
- [5] Manzoor, Alina, Muhammad Azhar Khan, Thamraa Alshahrani, M. H. Alhossainy, M. Sharif, Tariq Munir, Muhammad Imran Arshad, and M. Asif Iqbal. "Effect of Ho3+ ions on microwave losses and hightemperature electrical behavior of Li-based magnetic oxides." *Ceramics International* 47, no. 4 (2021): 4633-4642.
- [6] Lin, Qing, Fang Yang, Qian Zhang, Kaimin Su, Huiren Xu, Yun He, and Jinpei Lin. "Mössbauer and Structure-Magnetic Properties Analysis of A y B1- y C x Fe2- x O4 (C= Ho, Gd, Al) Ferrite Nanoparticles Optimized by Doping." *Molecules* 28, no. 10 (2023): 4226.
- [7] Goya, Gerardo Fabían, T. S. Berquo, F. Coral Fonseca, and M. P. Morales. "Static and dynamic magnetic properties of spherical magnetite nanoparticles." Journal of applied physics 94, no. 5 (2003): 3520-3528.
- [8] Purwins, H-G., and A. Leson. "Magnetic properties of (rare earth) Al2 intermetallic compounds." *Advances in Physics* 39, no. 4 (1990): 309-403.
- [9] Gimaev, Radel R., Aleksei S. Komlev, Andrei S. Davydov, Boris B. Kovalev, and Vladimir I. Zverev. "Magnetic and electronic properties of heavy lanthanides (Gd, tb, dy, er, ho, tm)." *Crystals* 11, no. 2 (2021): 82.
- [10] Kolmakova, N. P., A. A. Sidorenko, and R. Z. Levitin. "Features of the magnetic properties of rare-earth intermetallides RMn 2 Ge 2." *Low Temperature Physics* 28, no. 8 (2002): 653-668.
- [11] Wu, Ruqian, Chun Li, A. J. Freeman, and C. L. Fu. "Structural, electronic, and magnetic properties of rare-earth metal surfaces: hcp Gd (0001)." *Physical Review B* 44, no. 17 (1991): 9400.
- [12] Sinnema, S., R. J. Radwanski, J. J. M. Franse, D. B. De Mooij, and K. H. J. Buschow. "Magnetic properties of ternary rare-earth compounds of the type R2Fe14B." *Journal of magnetism and magnetic materials* 44, no. 3 (1984): 333-341.
- [13] Alonso, J. A., M. T. Casais, M. J. Martínez-Lope, J. L. Martínez, and M. T. Fernández-Díaz. "A structural study from neutron diffraction data and magnetic properties of (R= La, rare earth)." *Journal of Physics: Condensed Matter* 9, no. 40 (1997): 8515.
- [14] Koehler, W. C., E. O. Wollan, and M. K. Wilkinson. "Neutron diffraction study of the magnetic properties of rare-earth-iron perovskites." *Physical Review* 118, no. 1 (1960): 58.

- [15] Mansuripur, Masud, and M. Ruane. "Mean-field analysis of amorphous rare earth-transition metal alloys for thermomagnetic recording." *IEEE transactions on magnetics* 22, no. 1 (2003): 33-43.
- [16] Bud'ko, Sergey L., P. C. Canfield, C. H. Mielke, and A. H. Lacerda. "Anisotropic magnetic properties of light rare-earth diantimonides." *Physical Review B* 57, no. 21 (1998): 13624.
- [17] Xiang, Hongjun, Changhoon Lee, Hyun-Joo Koo, Xingao Gong, and Myung-Hwan Whangbo. "Magnetic properties and energy-mapping analysis." *Dalton Transactions* 42, no. 4 (2013): 823-853.
- [18] Naik, S. R., and A. V. Salker. "Change in the magnetostructural properties of rare earth doped cobalt ferrites relative to the magnetic anisotropy." *Journal of Materials Chemistry* 22, no. 6 (2012): 2740-2750.
- [19] Jacobo, S. E., S. Duhalde, and H. R. Bertorello. "Rare earth influence on the structural and magnetic properties of NiZn ferrites." *Journal of magnetism and magnetic materials* 272 (2004): 2253-2254.
- [20] Didchenko, R., and F. P. Gortsema. "Some electric and magnetic properties of rare earth monosulfides and nitrides." *Journal of Physics and Chemistry of Solids* 24, no. 7 (1963): 863-870.
- [21] Hansen, P., C. Clausen, G. Much, M. Rosenkranz, and K. Witter. "Magnetic and magneto-optical properties of rare-earth transition-metal alloys containing Gd, Tb, Fe, Co." *Journal of applied physics* 66, no. 2 (1989): 756-767.